A Cone-beam Reconstruction Algorithm for Dose-minimized Short Scan and Super Short Scan

Yan Xia, Frank Dennerlein, Sebastian Bauer, Martin Berger, Joachim Hornegger, and Andreas Maier

***Abstract*—Recently, we proposed an approach that deploys dynamic collimation to shield unnecessary redundant data in circular cone-beam data acquisition, enabling a dose-minimized short scan and super short scan. In this paper, we suggest a new reconstruction algorithm that produces images from these acquisitions that are superior to those restored by traditional short scan FDK-type algorithms. The method involves two stages: First, an initial volume was reconstructed by using a truncation correction method. However, this reconstruction suffers from the streaking artifacts in slices away from the mid-plane due to implicit sharp binary weighting to the cone-beam data. Then, we forward project this initial volume to fill the original projection areas that were shielded by collimation, so that a second reconstruction with a smooth Parker-weighting scheme can be applied to reduce the streaking effects. The evaluation is performed on clinical data with the simulated dose-minimized acquisition scans. The results demonstrate that the proposed algorithm achieves image quality that is comparable to non-collimated FDK short scan reconstruction, with minimized dose to the patient.**

I. Introduction

Today, clinicians typically rely on 3D C-arm CT imaging for interventional procedures in neuroradiology since 3D images offer more detailed anatomical information and higher low-contrast resolution than 2D angiography. 3D scans, however, cause a considerable amount of effective dose for a low-contrast scan of the patient's head [1]. Under such circumstances, it is the practical significance to reduce the radiation dose to the patient without compromising image quality.

There are many practical C-arm CT reconstruction algorithms that employ a weighting scheme (e.g., Parker weights [2]) to approximately compensate for the fact that during a partial circle scan some data are measured once, while other measurements are observed twice. In [3], we investigated the possibility to block redundant rays during the short scan acquisition by successively moving the collimator into the ray path at the beginning or end of the scan. We calculated that using this method the dose reduction for a C-arm CT with a fan angle of 20° is $10\,\%$, while for a diagnostic CT with a fan angle of 50° the reduction reaches $23\,\%$. Using dynamic collimation to shield redundant data is equivalent to applying a sharp binary weight. Direct use of this weight leads to large numerical errors due to its discontinuities, which was already demonstrated in [4]. To compensate these artifacts, we apply a robust truncation correction algorithm - Approximated Truncation Robust Algorithm for Computed Tomography (ATRACT) [5]. As shown in [3], ATRACT reconstructions from binary-weighted minimal complete data yields satisfying reconstruction results in mid-plane. But for slices away from the mid-plane, unacceptable streaking artifacts appear in the constructions due to the missing information in the cone-beam geometry.

In this paper, we present an approach that provides improved image quality even if only the binary-weighted minimal complete data is acquired. The basic idea of the algorithm is to forward project an initial reconstruction (with streaking artifacts for slices away from mid-plane) to fill the shielded areas in the original projection data, so that a second reconstruction with a smooth Parker-weighting scheme can be applied to reduce the streaking effects. Related work which deals with reducing streaking-like cone-beam artifacts proposed to blend the artifact-free parts of two initial volumes [6]. However, this blending is performed in frequency domain and the two initial volumes should fulfill some requirements. There also have been attempts involving an additional line, arc or helical scan [7], [8] to reduce streaking artifacts in cone-beam CT. But such an additional scan may complicate data acquisition and increase both the scan time and radiation dose.

II. Materials and Methods

A. Dose-Minimized Data Acquisition

The proposed algorithm deals with the reconstruction problem in recently suggested dose-minimized acquisition scans. Below, we briefly describe these scans.

1) Dose Saving in Short Scan : Let us first consider data redundancy in a short scan. As shown in Fig. 1b, the data in the triangle area ABC are redundant to the data in $A'B'C'$, which means only one triangle area must be acquired to reconstruct the object. In [3] we investigated the possibility to block redundant rays during short scan acquisition by successively moving the collimator into the ray path at the beginning or end of the scan. The angular interval of short scan is $\Lambda_s = [0, \pi + 2\delta]$, where $\delta = \arcsin(R/D)$. The resulting dose reduction γ_s can be theoretically estimated as the ratio between the short scan area and the collimated redundant area:

$$\gamma_s = \frac{\frac{1}{2}2\delta \cdot 4\delta}{2\delta\,(\pi + 2\delta)} = \frac{2\arcsin(R/D)}{\pi + 2\arcsin(R/D)}. \qquad (1)$$

Y. Xia, M. Berger, J. Hornegger and A. Maier are with the Pattern Recognition Lab, Friedrich-Alexander-University Erlangen-Nuremberg, 91058 Erlangen, Germany. Y. Xia and J. Hornegger are also with the Erlangen Graduate School in Advanced Optical Technologies (SAOT), Friedrich-Alexander-University Erlangen-Nuremberg, 91052 Erlangen, Germany. F. Dennerlein and S. Bauer are with Siemens AG, Healthcare Sector, Germany.

Disclaimer: The concepts and information presented in this paper are based on research and are not commercially available.

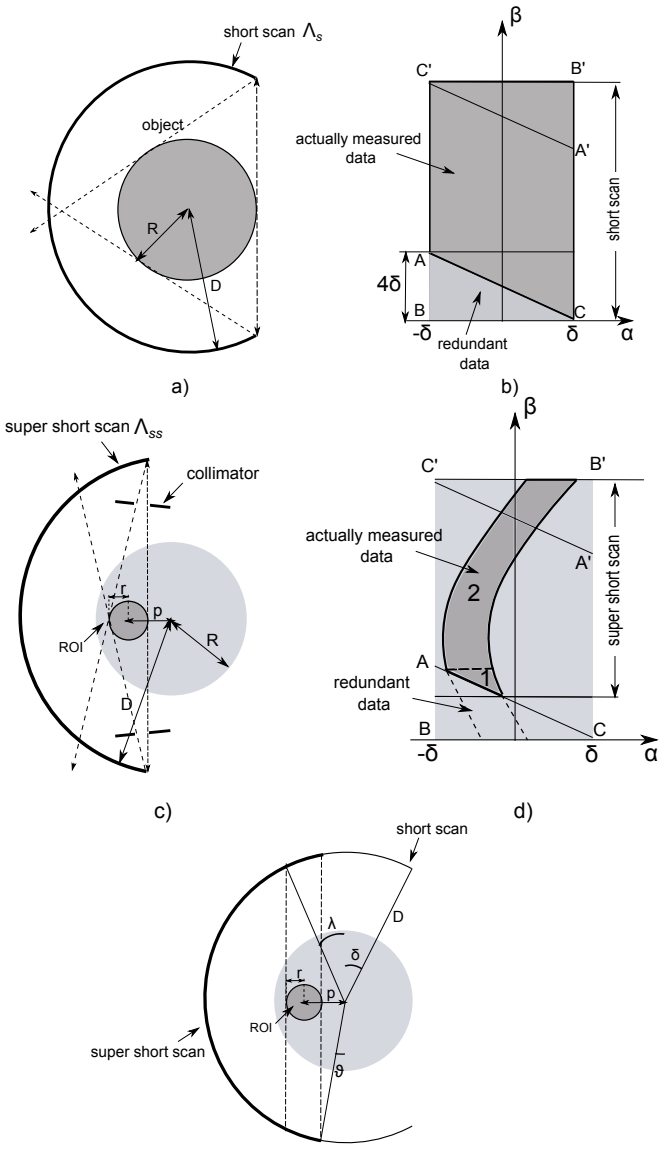

Figure 1. Illustration of the short scan and super short scan acquisition and the corresponding sinograms. a) and b): short scan with an angular interval $\Lambda_s = [0, \pi + 2\delta]$. c) and d): super short scan with an angular interval $\Lambda_{ss} = [0, \pi - 2\vartheta]$. e): potentially reduced angular range in a super short scan $(2\delta + 2\vartheta)$ as well as the angular range to acquire the area 1 $(2\lambda - 2\vartheta)$.

2) Dose Saving in Super Short Scan : A short scan acquisition is used when the entire object is to be reconstructed. However, the angular interval can be further reduced when only an ROI is required to be irradiated and reconstructed. Here we consider the off-center ROI shown in Fig. 1c. The centered ROI is just a special case when $p = 0$. When using collimation to get the truncated projections to reconstruct the specific ROI, we will only obtain the curved band in the sinogram (see Fig. 1d). However, the dashed curve band lies in the redundant region. Thus, the short scan angular range can be even further reduced and the acquisition can start at the point where the line AC intersects the ROI sinogram boundary since the scan segment below the intersect will be measured again at the area $A'B'C'$. We can apply an asymmetric collimation with changeable distance to acquire the area 1, followed by using an asymmetric collimation with fixed distance (shown in Fig. 1d) to acquire the area 2.

Figure 1e shows that the angular interval for super short scan is $\Lambda_{ss} = [0, \pi - 2\vartheta]$, where ϑ can be determined by the radius r and location p of the ROI:

$$\vartheta = \arcsin\left(\frac{p-r}{D}\right) . \tag{2}$$

With increasing distance from the iso-center and decreasing ROI radius, the angular interval decreases. Note that when the ROI is located at the iso-center ($p = 0$) and the radius of the ROI is equal to the object support ($r = R$), the interval above extends to the short scan range Λ_s. The dose reduction can be approximated by computing the ratio between the short scan range $\pi + 2\delta$ and the difference of short scan and super short scan range $2(\delta + \vartheta)$ plus half of the angular range to acquire the area 1 $(\lambda - \vartheta)$ (see Fig. 1e):

$$\gamma_{ss} = \frac{2\arcsin\left(\frac{R}{D}\right) + \arcsin\left(\frac{p-r}{D}\right) + \arcsin\left(\frac{p+r}{D}\right)}{\pi + 2\arcsin\left(\frac{R}{D}\right)} . \tag{3}$$

This gives the relationship between the radius r, location p of the ROI and potential dose reduction in a super short scan. For instance, for an off-centered ROI with radius $r = 20$ mm and location $p = 40$ mm acquired from a C-arm CT system with standard configuration $D = 750$ mm, $\arcsin(R/D) = 10°$, the potential dose reduction is $\gamma_{ss} = 13\,\%$.

B. New Streaking Reduction Algorithm

We present an approach that provides superior results with the minimal complete data acquired from a short scan or super short scan. The approach involves three steps. First, an initial volume is reconstructed using the ATRACT algorithm. However, this reconstruction suffers from streaking-like cone-beam artifacts in the slices away from mid-plane. Thus, we forward project the initially reconstructed volume and use the forward projections to fill the shielded areas in the original measured data. By doing so, we obtain artificial short scan data but at a lower radiation dose compared to an ordinary short scan. The last step in this pipeline is the FDK or ATRACT reconstruction with the standard Parker weights that will lead to the final reconstructed image with improved image quality, exhibiting substantially less streaking artifacts compared to the initially reconstructed volume. The flowchart of the algorithm is depicted in Fig. 2. Further details are elaborated in the following sections.

1) Initial Reconstruction : Blocking the redundant rays or acquiring ROI projections will result in truncated projection data, which is not compatible with conventional reconstruction algorithms. Here we apply a truncation robust algorithm (ATRACT) to deal with the truncation problem. The idea behind ATRACT is to adopt the FDK algorithm by decomposing the 1D ramp filter into two successive filter steps so that the filtering procedure is less sensitive to data truncation [5]. In this work we use a 1D version of ATRACT , in which the filtering step was adapted to a 1D Laplace filtering of the pre-weighted data and a 1D convolution-based filtering with a kernel $\ln|u|$ to get the filtered projection data [9]. It should

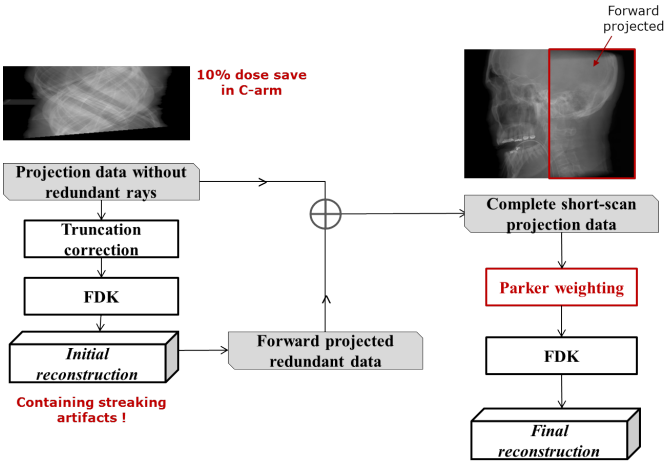

Figure 2. Flowchart of the proposed cone-beam reconstruction algorithm. First, an initial volume is reconstructed using the ATRACT algorithm. Then, we forward project the initially reconstructed volume and use the forward projections to fill the shielded areas in the original measured data. The last step involves the standard FDK algorithm or the ATRACT method, depending on complete projections or truncated ROI projections are processed.

be pointed out that the ATRACT algorithm yields accurate reconstructions in terms of truncation correction. However, as discussed before, streaking artifacts appear in off-center planes degrading image quality. That is why we propose a second reconstruction here, to compensate the streaking artifacts.

2) Forward projection: To perform the second reconstruction with improved image quality, it is necessary to complete the measured projections (truncated) with the information from the initial volume, so that a smooth weighting function (e.g, Parker weights) rather than the binary weighting, can be applied in the reconstruction to reduce the streaking effects. This requires the initial volume be forward projected in the original projection domain with the same detector size. In practice, the forward projection is only necessary to be performed on the redundant areas where original projections are shielded by collimation. These projections correspond to the triangle area ABC in Fig. 1b for a short scan and the dashed band in Fig. 1d for a super short scan.

3) Adaptive combination: The original dynamically-collimated data and the forward projected data are combined in the projection domain. Here an adjustment is needed to handle the incorrect forward projection values. To do so, an additional small overlapping region on the side of the original projection is also forward projected. Values are compared to the corresponding column of measured data in row-wise and a constant bias is added to the corresponding row in the forward projected data. Finally, the measured projections are filled by the transformed forward-projected data and the final image is reconstructed by the standard FDK algorithm or the ATRACT method, depending on the complete projections or truncated projections are processed.

C. Experimental Setup

To validate and evaluate the new method, two configurations were considered on a clinical human head dataset (data courtesy of St. Luke's Episcopal Hospital, Houston, TX, USA). The dataset was acquired on a C-arm CT system with 496 projections (1240×960 px) at the resolution of 0.308 mm / px.

In the first configuration, the short scan dataset was virtually cropped to mimic the removal of redundant area. The removed data correspond to the triangle area ABC in Fig. 1b. In configuration 2, we assume an off-centered ROI is reconstructed and the original short scan dataset was virtually collimated to the super short scan area that corresponds to area 1 and 2 in Fig. 1d. Note that the angular range in configuration 2 is 179°, which is much less than the standard short scan range of 200°.

The virtually collimated projections of both configurations were reconstructed onto a volume of $512 \times 512 \times 350$ voxels with an isotropic size of $0.45\,\mathrm{mm}^3$. The standard FDK reconstruction of the original short scan was used as the reference in each case. The data from configuration 1 and 2 were reconstructed by the proposed algorithm.

To quantify the improved accuracy obtained by the proposed algorithm, two quantitative metrics were used: the Root Mean Square Error (RMSE) and the Structural Similarity Index Measurement (SSIM) [10]. The SSIM measures the similarity of two volumes f_x and f_Ref and is calculated as follows:

$$\mathrm{SSIM}(f_\mathrm{x}, f_\mathrm{Ref}) = \frac{(2\mu_\mathrm{x}\mu_\mathrm{Ref} + c_1)(2\sigma_{\mathrm{x,Ref}} + c_2)}{(\mu_\mathrm{x}^2 + \mu_\mathrm{Ref}^2 + c_1)(\sigma_\mathrm{x}^2 + \sigma_\mathrm{Ref}^2 + c_2)}\,, \quad (4)$$

where μ_x and μ_Ref indicate the mean values of f_x and f_Ref, σ_x^2 and σ_Ref^2 indicate the variances of f_x and f_Ref and $\sigma_{\mathrm{x,Ref}}$ indicates their covariance. c_1 and c_2 are two constants to stabilize the results in case the denominator is too small (in our case, $c_1 = c_2 = 0$).

III. Results

The reconstruction results of the clinical dataset with configuration 1 are presented in Fig. 3. As expected, slight streaking artifacts are observed in the initial volume where ATRACT algorithm is applied. These streaking artifacts are oriented along a fixed direction associating with the truncated edge of the sinogram. In contrast, we found that the new algorithm yields almost identical image quality to the short scan FDK. The quantitative analysis in Table I also confirms the improvement of the proposed method: an RMSE of 28.3 HU is achieved compared to a larger error in the initial reconstruction (RMSE of 95.2 HU). It seems that the streaking artifacts do less impact on the structural similarity: both reconstructions yield similar SSIM results. Figure 4 shows two off-mid planes as well as a mid-plane of the ROI reconstructions with a super short scan. We can see that ATRACT (second column) is able to obtain high image quality in terms of truncation correction. No truncated-related bright ring or cupping artifacts are found within the FOV. Quantitative analysis with a SSIM of 0.93 also demonstrates this visual inspection. Note that reconstructing severely truncated data is an under-determined problem and the reconstructions will be biased by a constant. This explains the larger values in RMSE. Again, the streaking effect appears in slices that are away from the mid-plane. In contrast, no significant difference within the FOV is found between the proposed method and the reference, even in the off mid-planes.

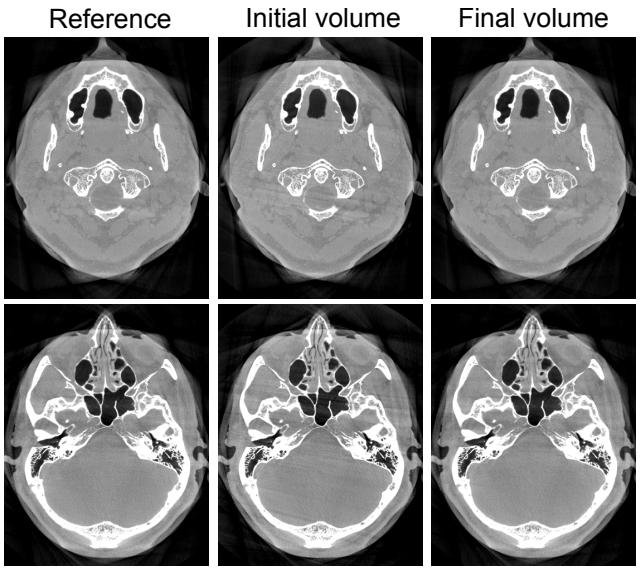

Figure 3. Reconstruction results of the binary-weighted short scan data by the proposed algorithm, in the gray scale window [-1000 HU, 1000HU]. Top row: z = 21.6 mm; bottom row: z = -21.6 mm.

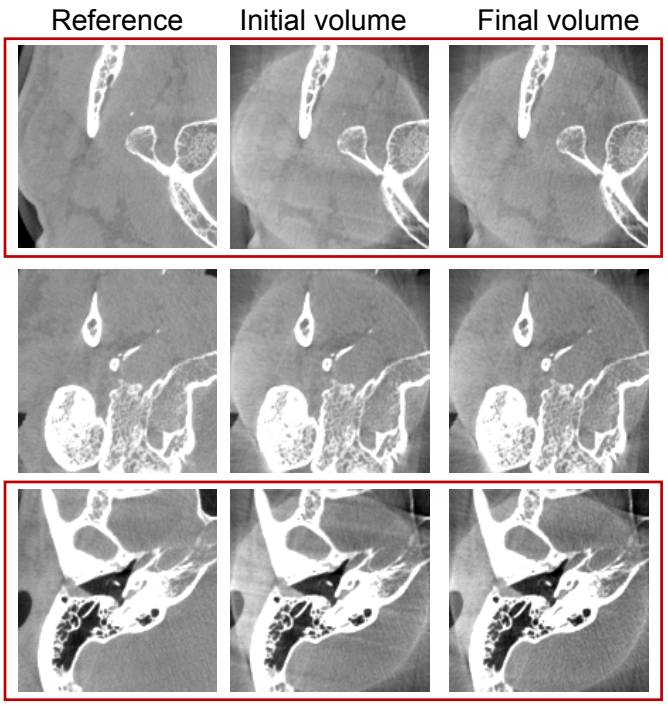

Figure 4. ROI reconstruction results of the binary-weighted super short scan data by the proposed algorithm, in the gray scale window [-1000 HU, 1000HU]. Top row: z = 26 mm; middle row: z = 0 mm; bottom row: z = -26 mm.

IV. Discussion

The experimental results show that our newly proposed algorithm yields improved image quality for the dose-minimized short scan and super short scan data. The amount of dose reduction in short scan depends on the fan-beam angle, with up to $10\,\%$ for C-arm CT and up to $23\,\%$ for diagnostic CT. In super short scan, dose saving additionally depends on the position and radius of the ROIs. When the ROI in Fig. 1c is located at the right side of the patient, the dose saving potential could also be kept by either shifting the scan trajectory to the right side of the patient or laterally moving the table to left direction so that the right ROI is repositioned in the left side. For a standard C-arm CT system, the latter seems to be more feasible than the former.

	Stage	RMSE (HU)	SSIM
Config 1	Initial volume	95.2	0.98
	Final volume	28.3	0.99
Config 2	Initial volume	160	0.93
	Final volume	155	0.94

Table I
Summary of quantitative evaluation in two experimental configurations.

Future work involves to further reduce computational complexity. It would be interesting to adapt the method proposed in [11]: since both measured minimal complete data and forward projected data are 2D entities, suggesting an approach that calculates the missing data directly from the original measured projections using 2D image processing steps, rather than explicitly performing reconstruction and forward projection. The computational complexity to estimate the missing data is considerably decreased, which will further deliver the algorithm to practical use.

Acknowledgment

The authors gratefully acknowledge funding by Siemens AG, Healthcare Sector and of the Erlangen Graduate School in Advanced Optical Technologies (SAOT) by the German Research Foundation (DFG) in the framework of the German excellence initiative.

References

[1] R. Fahrig, R. Dixon, T. Payne, R. L. Morin, A. Ganguly, and N. Strobel, "Dose and image quality for cone-beam C-arm CT system," *Medical Physics*, vol. 33, no. 12, pp. 4541–4550, 2006.

[2] D. L. Parker, "Optimal short scan convolution reconstruction for fan-beam CT," *Medical Physics*, vol. 9, pp. 254–257, 1982.

[3] Y. Xia, M. Berger, C. Riess, J. Hornegger, and A. Maier, "Dose Reduction Achieved by Dynamically Collimating the Redundant Rays in Fan-beam and Cone-beam CT," in *Proc IEEE NSS/MIC*, 2013, to appear.

[4] A. Naparstek, "Short-scan fan-beam algorithms for CT," *IEEE Trans. Nucl. Sci.*, vol. 27, pp. 1112–1120, 1980.

[5] F. Dennerlein and A. Maier, "Approximate truncation robust computed tomography - ATRACT ," *Physics in Medicine and Biology*, vol. 58, pp. 6133–6148, 2013.

[6] J. D. Pack, Z. Yin, K. Zeng, and E. N. Brian, "Mitigating cone-beam artifacts in short-scan CT imaging for large cone-angle scans," in *Proc Fully 3D 2013*, 2013, pp. 300–303.

[7] A. Katsevich, "Image reconstruction for the circle and line trajectory," *Physics in Medicine and Biology*, vol. 49, pp. 5059–5072, 2004.

[8] C. Bontus, P. Koken, T. Kohler, and R. Proksa, " Circular CT in combination with a helical segment," *Physics in Medicine and Biology*, vol. 52, pp. 107–120, 2007.

[9] Y. Xia, A. Maier, H. G. Hofmann, F. Dennerlein, K. Mueller, and J. Hornegger, "Reconstruction from truncated projections in cone-beam CT using an efficient 1D filtering," in *Proc SPIE*, 2013, 86681C.

[10] Z. Wang, A. C. Bovik, H. R. Sheikh, and E. P. Simoncelli, "Image quality assessment: from error visibility to structural similarity," *IEEE Transactions on Image Processing*, vol. 13, no. 4, pp. 600–612, 2004.

[11] F. Dennerlein, A. Jerebko, A. Fieselmann, and T. Mertelmeier, "Efficient Synthesis of Virtual Projections from a Tomosynthesis Data Set using a 2D Image Processing Method," in *Proc SPIE*, 2013, p. 86680W.